

Nonlinear Tracking Control Scheme for a Nanopositioner

Maridalena Vagia, Arnfinn A. Eielsen, J. Tommy Gravdahl and Kristin Y. Pettersen

Abstract—The ability to track periodic reference trajectory signals fast and with good accuracy, is highly required in many different nanopositioning applications. Since different factors can affect the performance of such devices, like lightly damped resonances and actuator nonlinearities including hysteresis and creep, a number of control schemes have been presented in order to overcome these difficulties, in the recent literature. In the present paper a nonlinear feedback controller is proposed that includes both force and tracking control of a nanopositioner. The nonlinear controller is an augmentation of a linear integral force controller where the constant gain used in the integral force feedback, is replaced by a passive nonlinear operator. The nonlinear control law provides improved performance with regards to disturbance rejection and vibration damping over the linear control law. In addition, a feedback component is added. The stability of the overall closed loop system is analysed using the multivariable Popov criterion.

I. INTRODUCTION

Nanodevices have been in the center of attention in the recent decades, because of their ability to be used in numerous applications in different scientific fields like biology, chemistry, materials science, and physics [1]. A typical application that nanopositioning devices are used for, is high resolution positioning. This, includes scanning probe microscopy (SPM) [2], [3], for both manipulation [4] and interrogation [5] at the nanometer scale.

Scanning probe microscopy requires one or more positioners to physically position the probe in space [6]. As such, high performance motion control is required. The motion can be generated using e.g. piezoelectric actuators [7], [8], electrostatic comb drives [9], or voice coil actuators [10], [11]. It is quite common for positioner designs to have high stiffness materials and as a result the positioner experiences little structural damping and in addition lightly damped vibrational modes. As a result, limitation of the bandwidth occurs since reference signals with high frequency components will excite the vibration modes. This is one of the main problems that can lead to non-accurate positioning. In addition, several other sources exist that introduce an uncertainty in the dynamic response of such systems. Nanopositioners are also susceptible to environmental disturbances, such as sound and floor vibrations. The list can get longer by adding uncertainties like hysteresis, and creep, that are loss-phenomena that

prevent the linear response. This will, in effect, introduce bounded disturbances dependent on the driving voltage [1].

For known signals, the effect of mechanical vibrations can be reduced by the application of different control techniques. Different techniques have been applied so far and even the simple application of feedforward controllers can lead to the desired results [12]. However, feedback control is more desirable since it is has been proven to be more efficient in reducing the sensitivity to unknown disturbances [13],[14]. Amongst the proposed feedback schemes that have been presented so far, one can find positive position feedback techniques [15], integral force feedback [16], passive shunt-damping [17], resonant control [18] and integral resonant control [19]. When it comes to nanoposition applications specifically, positive position feedback and resonant control has been applied in [20], integral force feedback in [21], passive shunt-damping in [22], [23], and integral resonant control in [24]. The main characteristics of these techniques are their simplicity in implementation and their robustness towards plant uncertainties and system nonlinearities.

The large majority of controllers proposed for nanopositioning systems in literature has been linear controllers based on linear models. However, linear control laws in have limitations to the achievable performance [25]. For a single-input-single-output system, this is perhaps most noticeable from the limitations imposed by the Bode sensitivity integral [26]. In [27] a nonlinear control approach was proposed in order to obtain performance improvement. In particular, the proposed control law replaces the constant gain controller that was previously presented by [16] with a passive nonlinear operator which includes a second-order term. The nonlinear control law improves the performance of the integral force feedback as it provides more rapid suppression of large disturbances, while maintaining low noise sensitivity, since the second-order term only provides high gain for large error signals. The stability properties of the closed loop system can be established using the theory of passivity [28].

In the present article this approach is taken a step forwards. Reference trajectory planning is applied for the closed loop system presented in [27] [13], [29]. Furthermore, we extend the control scheme applied in [27] with an extra feedback for displacement. As a result, a new closed loop system is derived for which tracking control is achieved using a feedforward control scheme. The stability of the closed loop system is analysed using of the multivariable Popov criterion as presented in [30], [31].

The paper is structured as follows: In Section II the nanopositioning system and the mathematical model is pre-

M. Vagia, A.A.Eielsen, J. T. Gravdahl and K. Y. Pettersen were with the Dept. of Engineering Cybernetics, Norwegian Univ. of Science and Technology, Trondheim, Norway. Corresponding author email: maridalena.vagia@sintef.no, M.Vagia was also with SINTEF IKT, Applied Cybernetics, Trondheim, Norway, A. A. Eielsen is now with the University of Newcastle (UON), Australia

sented. Section III presents the control scheme proposed, and Section IV theoretical proof of the stability of the control scheme. Finally in Section V simulation results are presented.

II. SYSTEM DESCRIPTION AND MODELLING

A. Description of the Experimental System

The overall applied nonlinear control law, is designed for the custom-made long-range serial-kinematic nanopositioner as presented in Fig. 1 [27]. The displacement is generated with a use of a piezoelectric actuator. Such actuators generate a force proportional to an applied voltage [33]. The piezoelectric actuator applies an external force f_a (N) the is equal to:

$$f_a = e_a u, \quad (1)$$

where e_a (N V⁻¹ = C N⁻¹) is the effective gain of the piezoelectric actuator from voltage to force, and u (V) is the applied voltage.

The dynamics of the structure due to an externally applied input voltage u for a point d (m) on the flexible structure, as observed by a co-located sensor, is adequately described by the following lumped parameter, truncated linear model [34],

$$G_d(s) = e_a \frac{y_d}{f_a}(s) \approx \sum_{i=1}^{n_d} \frac{\beta_i}{s^2 + 2\zeta_i \omega_i s + \omega_i^2} + D_r \quad (2)$$

n_d is the number of vibrational modes included. The other parameters are: $\{\beta_i\}$ (m s⁻² V⁻¹) the control gains, $\{\zeta_i\}$ the damping coefficients for each mode, and $\{\omega_i\}$ (rad s⁻¹) the natural frequencies for the modes. The term D_r (m V⁻¹) is the residual mode, which is an approximation of the non-modeled higher frequency modes, and can be included to improve prediction of zero-locations. The addition of D_r produces a model that is not strictly proper, but as the instrumentation, such as the amplifier and sensors, have limited bandwidth, D_r can be considered equal to zero for this system.

The integral force feedback controller scheme utilizes a co-located piezoelectric force transducer. The force transducer generates a charge, depending on the applied force. The current or charge produced by the force transducer is typically converted to a voltage signal using a simple op-amp circuit with a high input impedance. The output voltage from such a sensor when measuring the charge, can be found to be [21], [34]

$$y_f = k_s(k_a u - y_d),$$

where y_d is the displacement of the mechanical structure, u is the applied voltage to the actuator, k_a (m V⁻¹) is the gain of the feed-through term, and k_s (V m⁻¹) is the sensor gain. The transfer-function from applied voltage u_a to measured sensor voltage v_f can therefore be found as

$$G_f(s) = \frac{y_f}{u}(s) = k_s(k_a - G_d(s)). \quad (3)$$

For the displacement model (2), only the dominant vibration mode is included, i.e. $n_d = 1$. The dominant piston mode occurs at 1680 Hz.

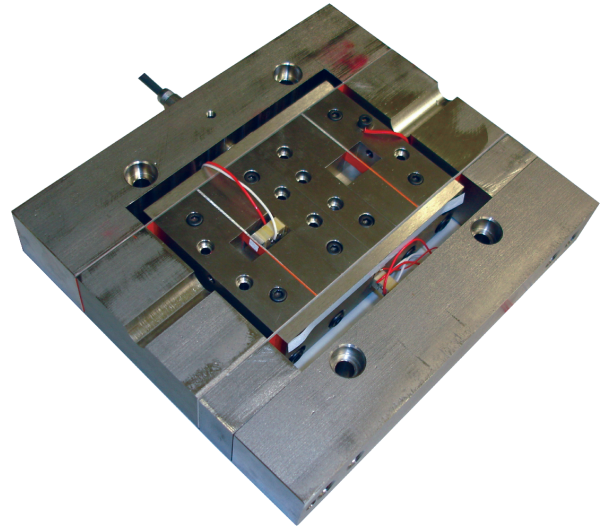


Fig. 1: Custom flexure-guided nanopositioning stage.

TABLE I: Identified model parameters.

Displacement model (2)		
β_1	$2.00 \cdot 10^6$	$\mu\text{m s}^{-2} \text{V}^{-1}$
ζ_1	0.0196	
ω_1	$2\pi \cdot 1680$	rad s ⁻¹
Force model (3)		
k_s	0.00197	V μm^{-1}
k_a	0.0253	$\mu\text{m V}^{-1}$

III. CONTROL SCHEMES

A. Integral Force Feedback and Nonlinear Control Schemes

Integral force feedback (IFF) was introduced in [16], and has successfully been applied to a nanopositioning device in [21]. An advantage of using this scheme, is that a piezoelectric force transducer typically has an extremely low noise density, compared to many other sensors [21]. The control law is also simple to tune and implement, and provides damping for several vibration modes simultaneously. Assuming sensor-actuator co-location, it provides robust \mathcal{L}_2 -stability.

The basic implementation of the control scheme is shown in Fig. 2a. Here

$$\Phi = k_2$$

and the IFF control scheme is therefore equivalent of the integral control law on the form

$$C(s) = \frac{k_2}{s}, \quad (4)$$

where k_2 is the control law gain.

The methodology for optimally tuning the linear gain k_2 is elaborately explained in [21], [35].

Linear control laws in general have limitations to the achievable performance [25]. For a single-input-single-output system, this is perhaps most noticeable from the limitations imposed by the Bode sensitivity integral [26]. For the IFF scheme, performance depends on the tuning for the gain

And therefore the feedback representation with the use of the linear integral controller is:

$$K_1 = \begin{bmatrix} 0 & 0 \\ 0 & k_2 \end{bmatrix}, \quad L_1 = \begin{bmatrix} 1 \\ -k_2 k_s k_a \end{bmatrix}$$

$$\underline{u} = -K_1 \underline{y} + L_1 r \quad (13)$$

$$\dot{\underline{x}} = (A_1 - B_1 K_1 C_1) \underline{x} + B_1 L_1 r$$

$$\underline{y} = (C_1 - D_1 K_1 C_1) \underline{x} + D_1 L_1 r$$

In this case r will function as the disturbance input.

$$u_1 = \begin{bmatrix} r \\ -k_2 \underline{y}_2 \end{bmatrix} = \begin{bmatrix} r \\ k_2 k_s \underline{x}_1 - k_2 k_s k_a \underline{x}_3 - k_2 k_s k_a r \end{bmatrix}$$

$$\begin{bmatrix} \dot{\underline{x}}_1 \\ \dot{\underline{x}}_2 \\ \dot{\underline{x}}_3 \end{bmatrix} = \begin{bmatrix} 0 & 1 & 0 \\ -\omega_1^2 & -2\zeta_1 \omega_1 & \beta_1 \\ k_2 k_s & 0 & -k_2 k_s k_a \end{bmatrix} \begin{bmatrix} \underline{x}_1 \\ \underline{x}_2 \\ \underline{x}_3 \end{bmatrix} + \begin{bmatrix} 0 \\ \beta_0 \\ -k_2 k_s k_a \end{bmatrix} r$$

$$\begin{bmatrix} \underline{y}_1 \\ \underline{y}_2 \end{bmatrix} = \begin{bmatrix} 1 & 0 & 0 \\ -k_s & 0 & k_s k_a \end{bmatrix} \begin{bmatrix} \underline{x}_1 \\ \underline{x}_2 \\ \underline{x}_3 \end{bmatrix} + \begin{bmatrix} 0 \\ k_s k_a \end{bmatrix} r$$

2) Case 2: Linear force and integral position feedback:

When the force feedback controller is added with the combination of the integral position feedback, if only the linear case is studied the state space representation of the open loop model will be examined with $a_1 = \omega_1^2$, $a_1 = 2\zeta_1 \omega_1$. Then, \bar{u}_1 is the first input to integrator \bar{x}_3 , and \bar{u}_2 is the second input to integrator \bar{x}_3 . Let us define \bar{u}_3 as the input to integrator \bar{x}_4 (reference input). No disturbance input is considered at this case.

$$\underbrace{\begin{bmatrix} \dot{\bar{x}}_1 \\ \dot{\bar{x}}_2 \\ \dot{\bar{x}}_3 \\ \dot{\bar{x}}_4 \end{bmatrix}}_{\bar{\dot{x}}} = \underbrace{\begin{bmatrix} 0 & 1 & 0 & 0 \\ -a_0 & -a_1 & \beta_0 & 0 \\ 0 & 0 & 0 & 0 \\ -1 & 0 & 0 & 0 \end{bmatrix}}_A \underbrace{\begin{bmatrix} \bar{x}_1 \\ \bar{x}_2 \\ \bar{x}_3 \\ \bar{x}_4 \end{bmatrix}}_x + \underbrace{\begin{bmatrix} 0 & 0 & 0 \\ 0 & 0 & 0 \\ 1 & -1 & 0 \\ 0 & 0 & 1 \end{bmatrix}}_B \underbrace{\begin{bmatrix} \bar{u}_1 \\ \bar{u}_2 \\ \bar{u}_3 \end{bmatrix}}_{\bar{u}}$$

$$\underbrace{\begin{bmatrix} \bar{y}_1 \\ \bar{y}_2 \\ \bar{y}_3 \end{bmatrix}}_{\bar{y}} = \underbrace{\begin{bmatrix} 1 & 0 & 0 & 0 \\ -k_s & 0 & k_s k_a & 0 \\ 0 & 0 & 0 & 1 \end{bmatrix}}_C \underbrace{\begin{bmatrix} \bar{x}_1 \\ \bar{x}_2 \\ \bar{x}_3 \\ \bar{x}_4 \end{bmatrix}}_x + \underbrace{\begin{bmatrix} 0 & 0 & 0 \\ 0 & 0 & 0 \\ 0 & 0 & 0 \end{bmatrix}}_D \underbrace{\begin{bmatrix} \bar{u}_1 \\ \bar{u}_2 \\ \bar{u}_3 \end{bmatrix}}_{\bar{u}}$$

In this case, \bar{y}_1 is the displacement, and \bar{y}_2 is the force. The output \bar{y}_3 is the integral of the displacement.

$$K_2 = \begin{bmatrix} 0 & k_2 & 0 \\ 0 & 0 & k_1 \\ 0 & 0 & 0 \end{bmatrix}, \quad L_2 = \begin{bmatrix} 0 \\ 0 \\ 1 \end{bmatrix}$$

$$\bar{u} = -K_2 \bar{y} + L_2 r = \begin{bmatrix} -k_2 \bar{y}_2 \\ -k_1 \bar{y}_3 \\ r \end{bmatrix} = \begin{bmatrix} k_2 k_s \bar{x}_1 - k_2 k_s k_a \bar{x}_3 \\ -k_1 \bar{x}_4 \\ r \end{bmatrix}$$

$$\underbrace{\begin{bmatrix} \dot{\bar{x}}_1 \\ \dot{\bar{x}}_2 \\ \dot{\bar{x}}_3 \\ \dot{\bar{x}}_4 \end{bmatrix}}_{\bar{\dot{x}}} = \underbrace{\begin{bmatrix} 0 & 1 & 0 & 0 \\ -a_0 & -a_1 & \beta_0 & 0 \\ k_2 k_s & 0 & -k_2 k_s k_a & k_1 \\ -1 & 0 & 0 & 0 \end{bmatrix}}_{\bar{A}_{cl}} \underbrace{\begin{bmatrix} \bar{x}_1 \\ \bar{x}_2 \\ \bar{x}_3 \\ \bar{x}_4 \end{bmatrix}}_{\bar{x}} + \underbrace{\begin{bmatrix} 0 \\ 0 \\ 0 \\ 1 \end{bmatrix}}_{\bar{B}_{cl}} r \quad (14)$$

$$\underbrace{\begin{bmatrix} \bar{y}_1 \\ \bar{y}_2 \\ \bar{y}_3 \end{bmatrix}}_{\bar{y}} = \underbrace{\begin{bmatrix} 1 & 0 & 0 & 0 \\ -k_s & 0 & k_s k_a & 0 \\ 0 & 0 & 0 & 1 \end{bmatrix}}_{\bar{C}_{cl}} \underbrace{\begin{bmatrix} \bar{x}_1 \\ \bar{x}_2 \\ \bar{x}_3 \\ \bar{x}_4 \end{bmatrix}}_{\bar{x}} + \underbrace{\begin{bmatrix} 0 \\ 0 \\ 0 \end{bmatrix}}_{\bar{D}_{cl}} r \quad (15)$$

3) Case 3: Nonlinear force and integral position feedback:

The final closed loop system as presented in Figure 2 will be presented in this case. The application of the Popov criterion requires that, $\bar{D}_{cl} = 0$. The system formulation of the Lure problem when using the Popov criterion is equal to:

$$\dot{x}_p = A_p x_p + B_p u_p$$

$$y_p = C_p x_p$$

$$u_p = -\Phi(y_p)$$

where $u_p = -\Phi(y_p)$ satisfies $u_{pi} = -\varphi_i(y_{pi})$, $i = 1, 2$.

$$\underbrace{\begin{bmatrix} \dot{\tilde{x}}_1 \\ \dot{\tilde{x}}_2 \\ \dot{\tilde{x}}_3 \\ \dot{\tilde{x}}_4 \end{bmatrix}}_{\tilde{\dot{x}}} = \underbrace{\begin{bmatrix} 0 & 1 & 0 & 0 \\ -a_0 & -a_1 & \beta_0 & 0 \\ 0 & 0 & 0 & 0 \\ -1 & 0 & 0 & 0 \end{bmatrix}}_{\tilde{A}} \underbrace{\begin{bmatrix} \tilde{x}_1 \\ \tilde{x}_2 \\ \tilde{x}_3 \\ \tilde{x}_4 \end{bmatrix}}_{\tilde{x}} + \underbrace{\begin{bmatrix} 0 & 0 \\ 0 & 0 \\ 1 & -1 \\ 0 & 0 \end{bmatrix}}_{\tilde{B}} \underbrace{\begin{bmatrix} \bar{u}_1 \\ \bar{u}_2 \end{bmatrix}}_{\tilde{u}}$$

$$\underbrace{\begin{bmatrix} \tilde{y}_1 \\ \tilde{y}_2 \end{bmatrix}}_{\tilde{y}} = \underbrace{\begin{bmatrix} -k_s & 0 & k_s k_a & 0 \\ 0 & 0 & 0 & 1 \end{bmatrix}}_{\tilde{C}} \underbrace{\begin{bmatrix} \tilde{x}_1 \\ \tilde{x}_2 \\ \tilde{x}_3 \\ \tilde{x}_4 \end{bmatrix}}_{\tilde{x}}$$

The input vector is now defined using the nonlinearity in (5).

$$\tilde{u} = -\tilde{K} \tilde{y} - \Phi(\tilde{y}) = \begin{bmatrix} -k_2 y_1 - \varphi_1(y_1) \\ -k_1 y_2 - \varphi_2(y_2) \end{bmatrix} = \begin{bmatrix} -k_2 y_1 \\ -k_1 y_2 \end{bmatrix} - \Phi(\tilde{y})$$

with $\tilde{u} = -\Phi(\tilde{y})$ and

$$\tilde{K} = \begin{bmatrix} k_2 & 0 \\ 0 & k_1 \end{bmatrix}$$

The closed loop system used for analysis is described by:

$$\underbrace{\begin{bmatrix} \dot{\tilde{x}}_1 \\ \dot{\tilde{x}}_2 \\ \dot{\tilde{x}}_3 \\ \dot{\tilde{x}}_4 \end{bmatrix}}_{\tilde{\dot{x}}} = \underbrace{\begin{bmatrix} 0 & 1 & 0 & 0 \\ -a_0 & -a_1 & \beta_0 & 0 \\ k_2 k_s & 0 & -k_2 k_s k_a & k_1 \\ -1 & 0 & 0 & 0 \end{bmatrix}}_{\tilde{A}_{cl}} \underbrace{\begin{bmatrix} \tilde{x}_1 \\ \tilde{x}_2 \\ \tilde{x}_3 \\ \tilde{x}_4 \end{bmatrix}}_{\tilde{x}} + \underbrace{\begin{bmatrix} 0 & 0 \\ 0 & 0 \\ 1 & -1 \\ 0 & 0 \end{bmatrix}}_{\tilde{B}_{cl}} \underbrace{\begin{bmatrix} \bar{u}_1 \\ \bar{u}_2 \end{bmatrix}}_{\tilde{u}} \quad (16)$$

$$\underbrace{\begin{bmatrix} \tilde{y}_1 \\ \tilde{y}_2 \end{bmatrix}}_{\tilde{y}} = \underbrace{\begin{bmatrix} -k_s & 0 & k_s k_a & 0 \\ 0 & 0 & 0 & 1 \end{bmatrix}}_{\tilde{C}_{cl}} \underbrace{\begin{bmatrix} \tilde{x}_1 \\ \tilde{x}_2 \\ \tilde{x}_3 \\ \tilde{x}_4 \end{bmatrix}}_{\tilde{x}} \quad (17)$$

$$\tilde{u} = -\Phi(\tilde{y}) = \begin{bmatrix} \bar{u}_1 \\ \bar{u}_2 \end{bmatrix} = - \begin{bmatrix} \varphi_1(y_1) \\ \varphi_2(y_2) \end{bmatrix} \quad (18)$$

IV. STABILITY ANALYSIS

The stability of the closed loop system presented above, is studied with the use of the multivariable Popov criterion [30], [31]. The closed loop system described has two different parts, a linear presented in Equations (16-17), and a nonlinear described in (18). The linear forward part, is described by a 4×4 matrix $W(s)$ of rational transfer functions which are equal to:

$$W(s) = C_{cl}(sI - A_{cl})B_{cl} \quad (19)$$

The feedback in this case is provided by the memoryless nonlinearities $\varphi_i(\tilde{y}_i), i = 1, 2 = \text{sat}((k_1|y_i|, L) + k_2)y_i, L, k_1, k_2 > 0, i = 1, 2$.

The closed loop system described in Equations (16-18) is stable and the stability proof is given below with the use of **Multivariable Popov Criterion** [30], [31]. The requirements that need to hold, in order for the system to be stable are:

Popov Criterion Requirements 1:

- 1) The $W(s)$ matrix of the rational transfer functions needs to be stable.
- 2) The memoryless nonlinearities need to satisfy the equations $0 \leq \varphi_i(\tilde{y}_i)\tilde{y}_i \leq k_i\tilde{y}_i^2, i = 1, 2$
- 3) There exist diagonal matrices $\hat{A} = \text{diag}\{a_1, a_2\}, \hat{B} = \text{diag}\{b_1, b_2\}$ with $a_i \geq 0, b_i \geq 0, i = 1, 2$ and $-a_i/b_i$ not a pole of any of the i th row elements of $W(s)$, such that will make the following function positive real:

$$Z(s) = (\hat{A} + \hat{B}s)W(s)$$

For the given case, the $W(s)$ matrix as described in Equation 19 is stable. In addition, the systems nonlinearities satisfy the property of Input Strict Passivity:

$$\varphi(y_i)y_i = \text{sat}((k_1|y_i|, L) + k_2)y_i^2 \geq k_2y_i^2$$

Graphically, the above presented result means that the nonlinearity belongs to the sector $[k_2, \infty]$. Finally, there exist two diagonal matrices \hat{A} and \hat{B} , so that the $Z(s)$ transfer function is positive real. Therefore all of the above conditions are fulfilled and finally, the nonlinear system, (16-18) is stable and the systems tracking properties are satisfied.

V. SIMULATION RESULTS

A simulation study was performed using the mathematical model of the nanopositioner stage presented in Section II and the controller is designed for the second vibrational mode. The block diagrams of the systems used in the simulations are the ones that have been presented in Figures 2a, 2b and 2c for the linear, the nonlinear/combined nonlinear cases and the tracking controller design. The different approaches are presented in order to show the improvements that are achieved by the use of the proposed tracking controller approach. In this case the main objective of the authors is to show the ability to achieve tracking.

For the case where no tracking controller is implemented an external excitation signals is used, equal to a square wave of 100V with a frequency equal to 20Hz. In the case of the

tracking control scheme a triangle wave reference signal of $1 \mu\text{m}$.

The results presented in Figs.3 and 4 indicate that the nonlinear control law provides improved performance with regards to disturbance rejection and vibration damping over the linear control law. Fig. 3 shows a reduced overshoot and a faster settling time for the combined nonlinear control law. It is interesting to note that the measured force is larger in the nonlinear case, indicating that the nonlinear control law produces a larger actuation signal for the same disturbance compared to the linear control law.

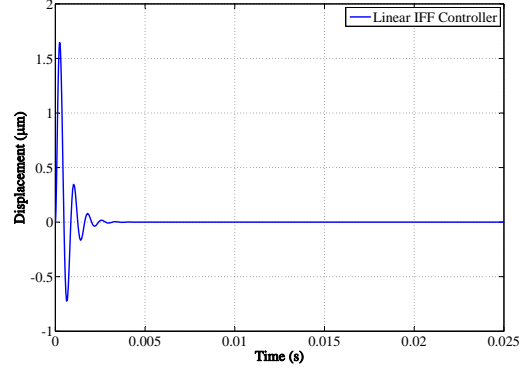


Fig. 3: Displacement Output for the pure linear controller scheme

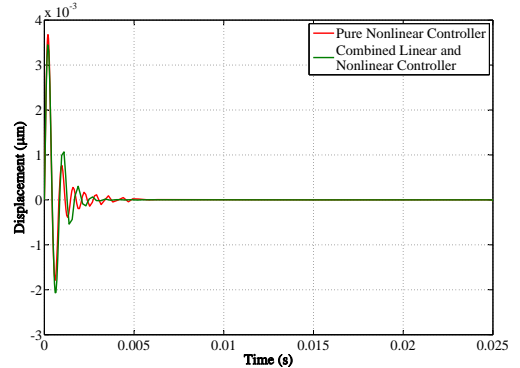


Fig. 4: Displacement Output for the pure nonlinear and the combined controller scheme

On the other hand, when the tracking controller is implemented the behaviour of the system changes according to what it is presented in Figures 6, and 7. Figures 6 present the output and the error of the nanopositioner closed loop system. From the results, it is shown that the applied controller leads the system to good tracking results. This is enforced by the error signal of the system, which clearly shows that its output follows with great accuracy the input signal. In addition, Figure 7 presents the measured sensor voltage output of the nonlinear tracking system as well.

VI. CONCLUSIONS

In the present paper, a nonlinear tracking feedback control scheme is presented for a nanopositioner. The nonlinear controller is an augmentation of a linear integral force controller where the constant gain used in the integral force feedback, is replaced by a passive nonlinear operator. An advantage of that scheme is that a piezoelectric force transducer typically has an extremely low noise density compared to other sensors. The stability of the overall closed loop system is analysed with the use of the multivariable Popov criterion, and the Simulation results prove the accuracy of the suggested scheme.

REFERENCES

- [1] S. Devasia, E. Eleftheriou, and S. O. R. Moheimani, "A Survey of Control Issues in Nanopositioning," *Control Systems Technology, IEEE Transactions on*, vol. 15, no. 5, pp. 802–823, 2007.
- [2] A. A. Tseng, S. Jou, A. Notargiacomo, and T. P. Chen, "Recent Developments in Tip-Based Nanofabrication and Its Roadmap," *Journal of Nanoscience and Nanotechnology*, vol. 8, no. 5, pp. 2167–2186, May 2008.
- [3] S. M. Salapaka and M. V. Salapaka, "Scanning Probe Microscopy," *Control Systems Magazine, IEEE*, vol. 28, no. 2, pp. 65–83, 2008.
- [4] M. Fuechsle, J. A. Miwa, S. Mahapatra, H. Ryu, S. Lee, O. Warschkow, L. C. L. Hollenberg, G. Klimeck, and M. Y. Simmons, "A single-atom transistor," pp. 1–5, Mar. 2012.
- [5] L. Gross, F. Mohn, N. Moll, P. Liljeroth, and G. Meyer, "The Chemical Structure of a Molecule Resolved by Atomic Force Microscopy," *Science*, vol. 325, no. 5944, pp. 1110–1114, Aug. 2009.
- [6] K. Fleming, A. J. and Leang, Kam, *Design, Modeling and Control of Nanopositioning Systems*, 1st ed. Springer, 2014.
- [7] G. Binnig and D. P. E. Smith, "Single-tube three-dimensional scanner for scanning tunneling microscopy," *Review of Scientific Instruments*, vol. 57, no. 8, pp. 1688–1689, 1986.
- [8] G. Schitter, P. J. Thurner, and P. K. Hansma, "Design and input-shaping control of a novel scanner for high-speed atomic force microscopy," *Mechatronics*, vol. 18, no. 5-6, pp. 282–288, 2008.
- [9] J. B. C. Engelen, H. E. Rothuizen, U. Drechsler, R. Stutz, M. Despont, L. Abelmann, and M. A. Lantz, "A mass-balanced through-wafer electrostatic x/y-scanner for probe data storage," *Microelectronic Engineering*, vol. 86, no. 4-6, pp. 1230–1233, June 2009.
- [10] H. Barnard, C. Randall, D. Bridges, and P. K. Hansma, "The long range voice coil atomic force microscope," *Review of Scientific Instruments*, vol. 83, no. 2, p. 023705 (4 pages), 2012.
- [11] T. Tuma, W. Haeberle, H. Rothuizen, J. Lygeros, A. Pantazi, and A. Sebastian, "A high-speed electromagnetically-actuated scanner for dual-stage nanopositioning," in *6th IFAC Symposium on Mechatronic Systems, Proceedings of the*, Hangzhou, Apr. 2013, pp. 125–130.
- [12] G. M. Clayton, S. Tien, K. K. Leang, Q. Zou, and S. Devasia, "A Review of Feedforward Control Approaches in Nanopositioning for High-Speed SPM," *Journal of Dynamic Systems Measurement and Control, Transactions of the ASME*, vol. 131, no. 6, p. 061101 (19 pages), 2009.
- [13] A. A. Eielsen, M. Vagia, J. T. Gravdahl, and K. Y. Pettersen, "Damping and Tracking Control Schemes for Nanopositioning," *IEEE/ASME International Conference on Advanced Intelligent Mechatronics, Proceedings of the*, pp. 1–13, 2013.
- [14] M. Vagia, "A frequency independent approximation and a sliding mode control scheme for a system of a micro-cantilever beam," *ISA transactions*, pp. 325–332, 2012.
- [15] J. L. Fanson and T. K. Caughey, "Positive Position Feedback-Control for Large Space Structures," *AIAA Journal*, vol. 28, no. 4, pp. 717–724, 1990.
- [16] A. Preumont, J. Dufour, and C. Malekian, "Active Damping by a Local Force Feedback with Piezoelectric Actuators," *Journal of Guidance Control and Dynamics*, vol. 15, no. 2, pp. 390–395, 1992.
- [17] N. W. Hagood and A. von Flotow, "Damping of Structural Vibrations with Piezoelectric Materials and Passive Electrical Networks," *Journal of Sound and Vibration*, vol. 146, no. 2, pp. 243–268, 1991.

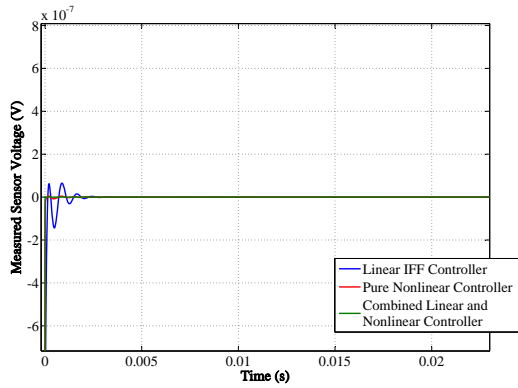


Fig. 5: Measured sensor voltage output for the pure linear, pure nonlinear and combined controller scheme

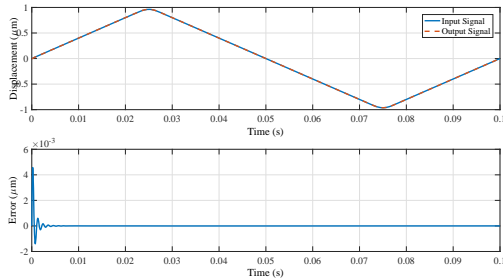


Fig. 6: System output for the tracking control scheme

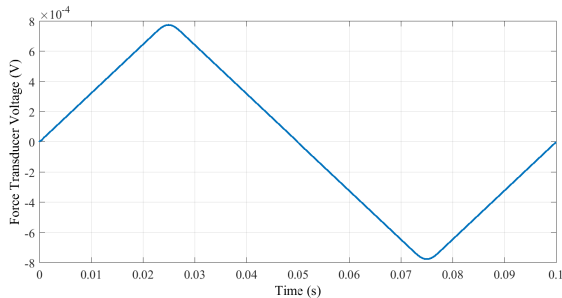


Fig. 7: Measured sensor voltage output for the tracking control scheme

- [18] H. Pota, S. O. R. Moheimani, and M. Smith, "Resonant Controllers for Smart Structures," *Smart Materials and Structures*, vol. 11, no. 1, pp. 1–8, 2002.
- [19] S. S. Aphale, A. J. Fleming, and S. O. R. Moheimani, "Integral Resonant Control of Collocated Smart Structures," *Smart Materials and Structures*, vol. 16, no. 2, pp. 439–446, 2007.
- [20] S. S. Aphale, B. Bhikkaji, and S. O. R. Moheimani, "Minimizing Scanning Errors in Piezoelectric Stack-Actuated Nanopositioning Platforms," *Nanotechnology, IEEE Transactions on*, vol. 7, no. 1, pp. 79–90, 2008.
- [21] A. J. Fleming, "Nanopositioning System With Force Feedback for High-Performance Tracking and Vibration Control," *Mechatronics, IEEE/ASME Transactions on*, vol. 15, no. 3, pp. 433–447, 2010.
- [22] M. W. Fairbairn, S. O. R. Moheimani, and A. J. Fleming, "Q Control of an Atomic Force Microscope Microcantilever: A Sensorless Approach," *Microelectromechanical Systems, Journal of*, vol. 20, no. 6, pp. 1372–1381, 2011.
- [23] A. A. Eielsens and A. J. Fleming, "Passive Shunt Damping of a Piezoelectric Stack Nanopositioner," in *American Control Conference, Proceedings of the*, Baltimore, MD, 2010, pp. 4963–4968.
- [24] B. Bhikkaji and S. O. R. Moheimani, "Integral Resonant Control of a Piezoelectric Tube Actuator for Fast Nanoscale Positioning," *Mechatronics, IEEE/ASME Transactions on*, vol. 13, no. 5, pp. 530–537, 2008.
- [25] S. Boyd and C. Barratt, *Linear Controller Design: Limits of Performance*. Prentice-Hall, 1991.
- [26] G. C. Goodwin, S. F. Graebe, and M. E. Salgado, *Control System Design*. Prentice Hall, 2000.
- [27] M. Vagia, A. Eielsens, J. Gravidahl, and K. Pettersen, "Design of a nonlinear damping control scheme for nanopositioning," in *Advanced Intelligent Mechatronics (AIM), 2013 IEEE/ASME International Conference on*, 2013, pp. 94–99.
- [28] B. M. B. Brogliato, R. Lozano and O. Egeland, *Dissipative Systems Analysis and Control*, 2nd ed. Springer, 2006.
- [29] G. Y. Gu, L. M. Zhu, and C. Y. Su, "High-precision control of piezoelectric nanopositioning stages using hysteresis compensator and disturbance observer," *ISmart Materials and Structures*, vol. 23, pp. 105 007–1105 007–10, 2014.
- [30] J. B. Moore and B. D. O. Anderson, "Application of the multivariable Popov Criterion," *International Journal of Control*, pp. 345–353, 1967.
- [31] —, "A generalization of the Popov Criterion," *Journal of the Franklin Institute*, pp. 488–492, 1968.
- [32] K. K. Leang and A. J. Fleming, "High-Speed Serial-Kinematic SPM Scanner: Design and Drive Considerations," *Asian Journal of Control*, vol. 11, no. 2, pp. 144–153, 2009.
- [33] A. Preumont, *Mechatronics*. Springer, 2006.
- [34] —, *Vibration Control of Active Structures: An Introduction*, 2nd ed. Kluwer Academic Publishers, 2002.
- [35] A. Preumont, B. de Marneffe, A. Deraemaeker, and F. Bossens, "The damping of a truss structure with a piezoelectric transducer," *Computers & Structures*, vol. 86, no. 3-5, pp. 227–239, Feb. 2008.
- [36] R. K. Kanestrøm and O. Egeland, "Nonlinear Active Vibration Damping," *Automatic Control, IEEE Transactions on*, vol. 39, no. 9, pp. 1925–1928, 1994.